Progress In Electromagnetics Research M, Vol. 73, 25–35, 2018

A Novel Hybrid Fractal Antenna for Wireless Applications

Narinder Sharma[1, *], Vipul Sharma[2], and Sumeet S. Bhatia[3]

Abstract—This paper presents a hybrid design of Sierpinski Carpet and Minkowski antenna for wireless applications. The hybrid antenna is designed, simulated and fabricated on an FR4 substrate with thickness 1.6 mm and dielectric constant 4.4. The dimensions of antenna are $45 \times 38.92 \times 1.6\,\text{mm}^3$ which operates at various frequencies 3.43 GHz, 4.78 GHz, 6.32 GHz, 8.34 GHz and 9.64 GHz, and can be used for Wi-Max, C-band applications, Point-to-point Hi speed wireless communication and X-band (satellite Communication) applications. The measured results are also compared with the simulated ones which are in agreement with each other. Ansoft High Frequency Structure Simulator (HFSS) is used to design and simulate the antenna.

1. INTRODUCTION

In the field of wireless technology, there is a need to enhance the performance of wireless devices in the area of voice and data communication. The development of various wireless communication devices focuses on the compact size, light weight, wide bandwidth for high data rate, etc. [1, 2]. Antenna design plays a vital role in wireless communication especially with its small size, simple structure and multiband or wideband characteristics. To achieve the multiple standards in a single device is a very crucial task for the designers. Fractal shapes have created revolution in the design and development of multiband antennas [3]. Various types of fractal geometries have been proposed by different researchers for the development of wideband and multiband antennas [4]. In 1975, Mandelbort was the first to introduce the fractal geometry, in which the whole geometry repeats itself by a particular scale in different iterations [5, 6]. Fractal shapes are generated by using recursive procedures which produce large surface area in limited space [7, 8]. So, geometries and dimensions of fractal structures are important deciding factor for the operative resonant frequencies [9]. Self similarity and space filling is key properties of fractal geometries used in designing fractal antennas [10, 11]. The self similarity of fractal shapes can be obtained by applying the infinite number of iterations with the help of Multiple Reduction Copy Machine (MRCM) algorithm [12, 13], and it also helps the antenna to achieve multiband characteristics. The space filling property is used to reduce the size of antenna or to achieve the miniaturization of antenna [14]. The miniaturization of antenna is achieved by increasing the effective permeability and permittivity of the substrate [15]. It has been observed from the discussed literature survey that an optimal hybrid of Minkowski and Sierpinski Carpet antennas can be designed for the wireless communication.

So, a hybrid fractal antenna is designed by combining Minkowski curve with indention angle (θ) 90° and rectangular Sierpinski carpet fractal geometry. The geometric shape of Minkowski curve is designed by taking the straight line (initiator) which is shown in Fig. 1(a), and the generator structure is shown in Fig. 1(b). The recursive procedure is repeated up to 2nd iteration as shown in Fig. 1(c), to

Received 24 May 2018, Accepted 23 August 2018, Scheduled 4 September 2018
* Corresponding author: Narinder Sharma (dr.narinder.sharma0209@gmail.com).
[1] ECE, Amritsar College of Engineering, Amritsar, Punjab, India.
[2] ECE, Gurukul Kangri University, Haridwar, Uttrakhand, India. [3] Yadavindra College of Engineering, Punjabi University, Guru Kashi Campus, Talwandi Sabo, Bathinda, Punjab, India.

obtain the required Minkowski fractal shape by using Iterated Function System (IFS) which is discussed in Section 2, and its dimensions are computed [16] as:

$$\text{Indentation factor } (\rho) = \frac{h}{W_P/3} \tag{1}$$

where h is the indentation depth, and $W_p/3$ is the fractional part of W_p.

This manuscript comprises four sections. Section 1 demonstrates the introduction of antenna and extensive literature survey required for designing of proposed antenna. In the end of Section 1, fusion of Minkowski and Sierpinski geometries is also explained. Section 2 is based on iterative function system which is prominently used for designing the proposed antenna geometry. Section 3 explains the detailed antenna design along with the required configuration; this section elaborates the proper design steps of designed antenna. Section 4 reports the results of proposed antenna in the text as well as tabular form. To validate the novelty of antenna, the proposed antenna is also juxtaposed with the existing antennas stated in the art of literature in this manuscript.

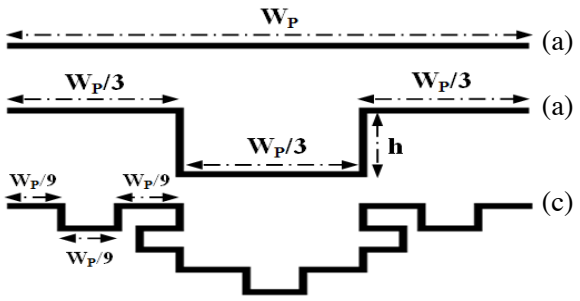

Figure 1. (a) Initiator geometry, (b) generator geometry and (c) proposed Minkowski curve.

2. IFS — ITERATED FUNCTION SYSTEM

Fractals are usually composed of sum of their own copies, whereas certain fractals are also made up by using the iterative procedures, and this procedure is generally said as Iterated Function System (IFS). IFS is a versatile mathematical tool, which is extremely useful when constructing the fractal geometries. It simply works by applying series of affine transformations (W) to an elementary shape (A). Affine transformation comprises scaling, translation and rotation and is represented as:

$$W(x) = Ax + t = \begin{bmatrix} a & b \\ c & d \end{bmatrix} \begin{bmatrix} x_1 \\ x_2 \end{bmatrix} \begin{bmatrix} e \\ f \end{bmatrix} \tag{2}$$

where matrix A (initial geometry) is given as:

$$A = \begin{bmatrix} (1/s)\text{Cos}\theta & -(1/s)\text{Sin}\theta \\ (1/s)\text{Sin}\theta & (1/s)\text{Cos}\theta \end{bmatrix} \tag{3}$$

where x_1, x_2 — Coordinates of point x; s — Scaling factor; θ — Rotation angle; t — Translation factor; a, b, c, d, e and f are the real numbers.

Here a, b, c and d are used to control the rotation and scaling, whereas e and f are used to control the linear shift and translation [17].

W is also known as Hutchinson operator, on applying set of transformations on A as:

$$W(A) = \bigcup_{n=1}^{N} W_N(A) \tag{4}$$

Using the Hutchinson Operator (W), we will obtain fractal geometry. The transformations to get the

segments of generator of our obtained Minkowski geometry are as [18]:

$$W_1(x) = \begin{bmatrix} 0.333 & 0 \\ 0 & 0.333 \end{bmatrix} \left(\frac{x_1}{x_2}\right) + \begin{bmatrix} 0 \\ 0 \end{bmatrix} \tag{5}$$

$$W_2(x) = \begin{bmatrix} 0 & 0.200 \\ -0.200 & 0 \end{bmatrix} \left(\frac{x_1}{x_2}\right) + \begin{bmatrix} 0.333 \\ 0 \end{bmatrix} \tag{6}$$

$$W_3(x) = \begin{bmatrix} 0.333 & 0 \\ 0 & 0.333 \end{bmatrix} \left(\frac{x_1}{x_2}\right) + \begin{bmatrix} 0.333 \\ -0.200 \end{bmatrix} \tag{7}$$

$$W_4(x) = \begin{bmatrix} 0 & -0.200 \\ 0.200 & 0 \end{bmatrix} \left(\frac{x_1}{x_2}\right) + \begin{bmatrix} 0.666 \\ -0.200 \end{bmatrix} \tag{8}$$

$$W_5(x) = \begin{bmatrix} 0.333 & 0 \\ 0 & 0.333 \end{bmatrix} \left(\frac{x_1}{x_2}\right) + \begin{bmatrix} 0.666 \\ 0 \end{bmatrix} \tag{9}$$

where W_1, W_2, W_3, W_4, and W_5 are the set of affine linear transformations. The generator is obtained as:

$$W(A) = W_1(A) \cup W_2(A) \cup W_3(A) \cup W_4(A) \cup W_5(A) \tag{10}$$

3. ANTENNA DESIGN AND CONFIGURATION

Two different fractal geometries are fused together to design a hybrid fractal antenna for attaining multiband characteristics, and though single fractal geometry may show multiband characteristics, integration of two fractal geometries can exhibit better multiband characteristics. Keeping this under consideration the proposed antenna is designed, and its design steps are explained as:

In step 1 of the proposed antenna, a rectangular patch has been designed and shown in Fig. 2(a). For designing the rectangular patch, different design parameters have been taken into consideration such as resonant frequency of antenna 3.2 GHz, relative permittivity of substrate 4.4 and thickness of substrate (t) 1.6 mm. In this design, we use low cost and easily available FR4 glass epoxy material as a substrate for the designing and fabrication of antenna. The length (L_p) and width (W_p) of the rectangular patch are calculated by using the following equations [19]:

$$W_P = \frac{c}{2f_r\sqrt{\frac{\varepsilon_r + 1}{2}}} \tag{11}$$

where ε_r is the relative permittivity, f_r the resonant frequency, and c the velocity of light. The calculated value of W_P is 28.52 mm.

The Effective Dielectric Constant (ε_{reff}) can be calculated as:

$$\varepsilon_{reff} = \left[\frac{\varepsilon_r + 1}{2} + \frac{\varepsilon_r - 1}{2}\right] \frac{1}{\sqrt{1 + {}^{12h}/_{W_P}}} \tag{12}$$

The extended incremental length (ΔL) of antenna is calculated as:

$$\Delta L = h * 0.412 \left[\frac{(\varepsilon_{reff} + 0.3)\left(\frac{W_P}{h} + 0.264\right)}{(\varepsilon_{reff} - 0.258)\left(\frac{W_P}{h} + 0.8\right)}\right] \tag{13}$$

The actual Length (L_P) of patch is given by:

$$L_P = \frac{1}{2f_r\sqrt{\mu_o}\varepsilon_o\sqrt{\varepsilon_r}} - 2\Delta L \tag{14}$$

The calculated value of L_P is 21.92 mm.

In this design, a corporate feed line has been introduced in the antenna design for the proper match of 50 Ω microstrip feed line impedance. After designing the rectangular patch in step 1, nine rectangular

slots of length X_{S1}, X_{S2} ($L_P/9$) and width Y_{S1} ($W_P/9$) have been etched from the rectangular patch in step 2, resulting into analogous Sierpinski Carpet geometry and depicted in Fig. 2(b). The computed value of X_{S1} and X_{S2} is 3.16 mm, whereas width Y_{S1} is 2.43 mm. The antenna shown in Fig. 2(b) is a single iteration of Sierpinski fractal antenna. Next iterations can also be taken, but for the sake of simplicity of the design, it is constrained to single iteration in this manuscript. Further, in step 3, width of rectangular patch is taken same as length of initiator of Minkowski curve illustrated in Fig. 1(a), and then generator geometry of Minkowski curve adorned in Fig. 1(b) with indentation depth (h) has been superimposed on the geometry of antenna indicated in Fig. 2(b) to attain the antenna design limned in Fig. 2(c). Similarly, to obtain the geometry of proposed antenna 1 elaborated in Fig. 2(d), the 2nd iteration of Minkowski curve illustrated in Fig. 1(c) is integrated on the geometry embellished in step 3 to design hybrid antenna. Proposed antenna 2 has been designed to improve the performance of proposed antenna 1. In antenna 2, four rectangular slots with width B_1 and length A_1 have been etched from the vertical sides of the rectangular patch reported in Fig. 2(d). The geometries of proposed antenna 1 and antenna 2 with dimensions are illustrated in Figs. 3(a) and 3(b), and their parametric values are delineated in Table 1.

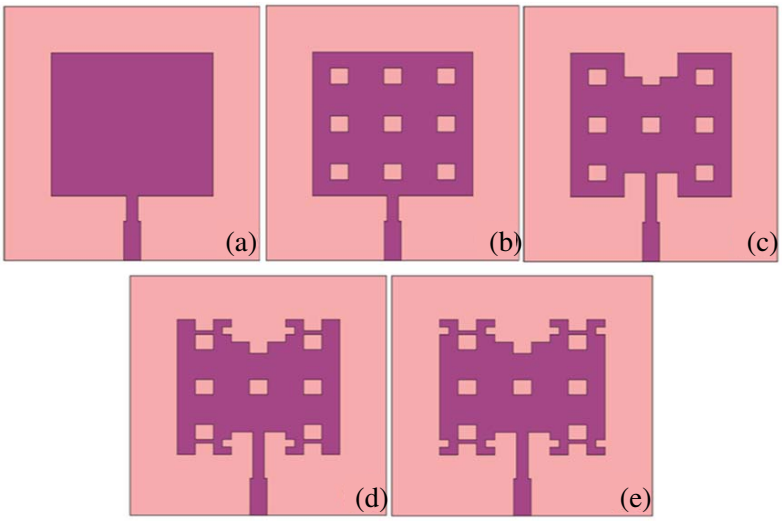

Figure 2. Design steps of proposed antenna: (a) step 1, (b) step 2 (analogous Sierpinski carpet), (c) step 3, (d) proposed antenna 1 and (e) proposed antenna 2.

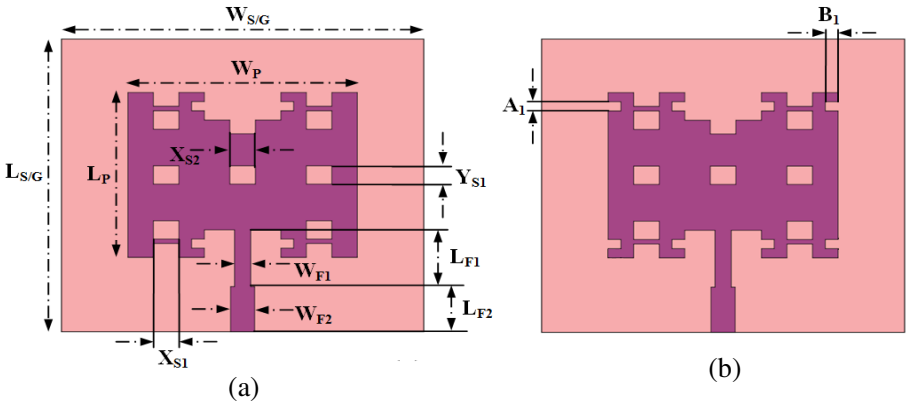

Figure 3. Dimensional geometry of hybrid fractal antenna: (a) proposed antenna 1 and (b) proposed antenna 2.

Table 1. Dimensions of the geometry of proposed antenna 1 and 2.

Antenna design parameters	Description	Dimensions
L_P	Length of patch	21.92 mm
W_P	Width of patch	28.52 mm
$W_{S/G}$	Width of substrate and ground plane	45 mm
$L_{S/G}$	Length of substrate and ground plane	38.92 mm
X_{S1}	Width of sierpinski slot	3.168 mm
X_{S2}	Width of sierpinski slot	3.168 mm
Y_{S1}	Length of sierpinski slot	2.435 mm
W_{F1}	Width of upper feed line	2.0 mm
L_{F1}	Length of upper feed line	7.54 mm
W_{F2}	Width of lower feed line	3.0 mm
L_{F2}	Length of lower feed line	6.0 mm
A_1	Length of vertical side slot	1.21 mm
B_1	Width of vertical side slot	1.58 mm

4. RESULTS AND DISCUSSIONS

The results of antenna depicted in Fig. 2 are explained as:

Antenna design in Fig. 2(a) exhibits tetravalent frequency bands and multiband behavior with corresponding reflection coefficient −12.77 dB at 3.17 GHz, −13.81 dB at 4.88 GHz, −16.49 dB at 8.18 GHz and −16.95 dB at 9.21 GHz.

To improve the reflection coefficient, an antenna has been further modified by applying the two different fractal geometries as demonstrated in Figs. 2(b) and 2(c). After the fusion of Sierpinski and Minkowski fractal geometries, the resulted antenna is named as antenna 1 which again reports the tetravalent frequency band but with improved reflection coefficient. The reported reflection coefficients at distinct frequencies are −19.37 dB at 3.41 GHz, −32.08 dB at 4.76 GHz, −13.11 dB at 6.28 GHz and −14.93 dB at 8.33 GHz.

It has been observed from the results of proposed antenna 1 that the reflection coefficient of lower frequency bands has been improved, and higher frequency bands have been shifted towards the lower side which may lead to miniaturization of the antenna. Further, to increase the number of frequency bands as well as improvement in the reflection coefficient, rectangular slots have been introduced in the geometry of proposed antenna 1 to obtain the geometry of proposed antenna 2. It has been observed that proposed antenna 2 reports one additional frequency band 9.61 GHz with corresponding reflection coefficient −17.57 along with other four frequency bands 3.43 GHz, 4.78 GHz, 6.32 GHz and 8.34 GHz. The comparison of reflection coefficient versus frequency curve of the proposed antennas along with the antenna designed in step 1, step 2 and step 3 is depicted in Fig. 4. Simulated results of all the antennas are compared in Fig. 4 and tabulated in Table 2 for more lucidity.

The aforementioned hybrid antennas (Proposed antennas 1 and 2) are simulated and fabricated to find the performance parameters such as return loss, VSWR, radiation pattern and gain. The simulated antenna 1, shown in Fig. 3(a), exhibits four frequency bands, i.e., 3.41 GHz, 4.76 GHz, 6.28 GHz and 8.33 GHz. To increase the operating frequency bands, the four rectangular slots have been extracted from vertical sides of the rectangular patch of proposed antenna 1 and named as proposed antenna 2, shown in Fig. 3(b). The simulated antenna-2 exhibits five frequency bands i.e., 3.41 GHz, 4.78 GHz, 6.32 GHz, 8.34 GHz and 9.61 GHz.

To validate the simulated results, aforementioned simulated antennas are fabricated by using FR-4 substrate material. The fabricated hybrid antennas are shown in Figs. 5(a) and 5(b) and named as proposed antennas 1 and 2. These antennas are tested on Vector Network Analyzer (VNA-MS46322A,

Table 2. Comparison of simulated results of different geometries of proposed antennas.

Antenna design	Frequency (GHz)	Reflection Coefficient (dB)	VSWR	Radiation efficiency (%)
Step 1	3.17	−12.77	1.59	72.83
	4.88	−13.81	1.51	75.89
	8.18	−16.49	1.35	85.23
	9.21	−16.95	1.33	86.85
Step 2	3.11	−11.57	1.71	80.56
	4.81	−13.28	1.55	81.52
	8.05	−15.35	1.41	79.26
	8.92	−39.24	1.02	77.63
Step 3	3.33	−21.89	1.17	88.77
	4.88	−25.88	1.10	89.96
Proposed	3.41	−19.37	1.24	86.59
Antenna 1	4.76	−32.08	1.05	74.52
	6.28	−13.11	1.56	72.69
	8.33	−14.93	1.43	86.56
Proposed	3.43	−19.50	1.23	78.95
Antenna 2	4.78	−28.70	1.07	80.59
	6.32	−12.46	1.62	85.96
	8.34	−18.75	1.26	79.58
	9.61	−17.57	1.30	89.99

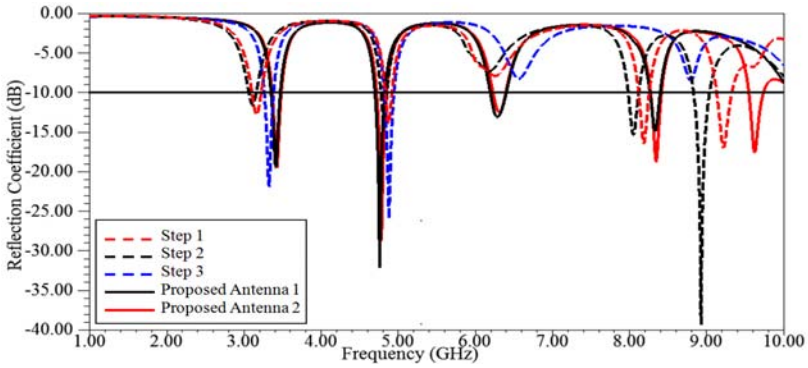

Figure 4. Comparison of reflection coefficient versus frequency curve of different geometries of proposed antennas.

Anritsu), to obtain the performance parameters such as return loss and VSWR. The measured frequency bands of antenna 1 are 3.48 GHz, 4.74 GHz and 8.38 GHz, whereas the frequency bands for antenna 2 are 3.48 GHz, 4.78 GHz, 8.30 GHz and 9.67 GHz. The frequency bands obtained from simulated antennas (shown in Fig. 3) and fabricated antennas (shown in Fig. 5) have return loss ($S_{11} \leq -10$ dB) and VSWR ≤ 2, which are acceptable for the practical use of antenna. These results exhibit a reasonable agreement although there is difference of one frequency band in simulated and measured antennas that can be attributed to reflection from SMA connector, environmental conditions, unwanted radiations and also some uncertainty in the electrical properties of the substrate. The comparison of measured

and simulated return losses vs frequency curve for antenna 1 and antenna 2 are reported in Fig. 6 and Fig. 7. The value of return loss and VSWR of measured and simulated antennas along with resonant frequency bands are shown in Table 3.

Table 3. Comparison of simulated and measured results of antenna-1 and antenna-2.

Antenna No.	Simulated				Measured			
	Frequency (GHz)	Reflection Coefficient (dB)	VSWR	Gain (dB)	Frequency (GHz)	Reflection Coefficient (dB)	VSWR	Gain (dB)
Proposed Antenna 1	3.41	−19.37	1.24	2.13	3.48	−26.70	1.09	1.98
	4.76	−32.08	1.05	5.04	4.74	−16.98	1.33	4.95
	6.28	−13.11	1.56	5.18	–	–	–	–
	8.33	−14.93	1.43	6.18	8.38	−25.09	1.11	5.89
Proposed Antenna 2	3.43	−19.50	1.23	2.84	3.48	−21.32	1.18	2.54
	4.78	−28.70	1.07	6.90	4.78	−19.60	1.23	6.10
	6.32	−12.46	1.62	5.13	–	–	–	–
	8.34	−18.75	1.26	5.57	8.30	−25.59	1.11	4.99
	9.61	−17.57	1.30	7.56	9.67	−18.02	1.28	7.01

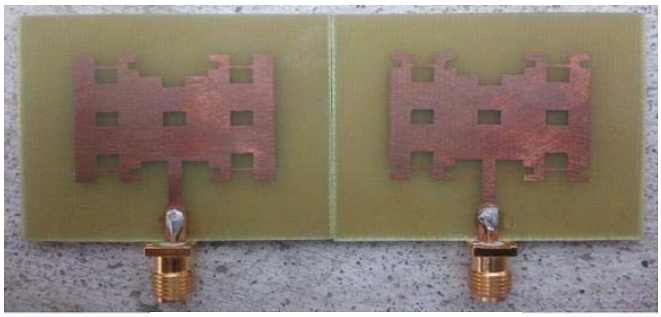

(a) (b)

Figure 5. Fabricated prototype of (a) proposed antenna-1 and (b) proposed antenna-2.

Radiation pattern is a graphical representation of the relative field strength of radio waves from antenna or any other sources. This is represented in polar or rectilinear form and measured in dB. In the case of fractal antenna, the useful portion of radiation pattern will be elevation plane for $\varphi = 0°$and $\varphi = 90°$ [20]. Figs. 8(a) to (e) indicate the 2-D far-field radiation pattern for each frequency band of proposed antenna 2. These figures also depict omnidirectional properties of the proposed antenna. Fig. 8(f) shows the 3-D gain plot for maximum value, i.e., 7.60 dB at resonant frequency 9.64 GHz, which is an acceptable level as per the requirement of fractal antennas. Gains of proposed antenna 1 and antenna 2 have also been measured and juxtaposed with the simulated gains and anticipated in Fig. 9. The values of simulated and measured gains of the proposed antennas are also delineated in Table 3 for more clarity. Comparison of results obtained from the proposed antenna is made with published work as shown in Table 4.

It can be observed form Table 3 that the proposed hybrid antenna is optimal, as it is compact in size in comparison to mentioned papers except [15] and [22], but if we visualize [15], it operates at only one resonant frequency with gain 1.67, whereas that in [22] operates on two resonant frequencies with gain 1.8/2.4. So, we can say that the proposed antenna works on multiple resonant frequencies with high gain.

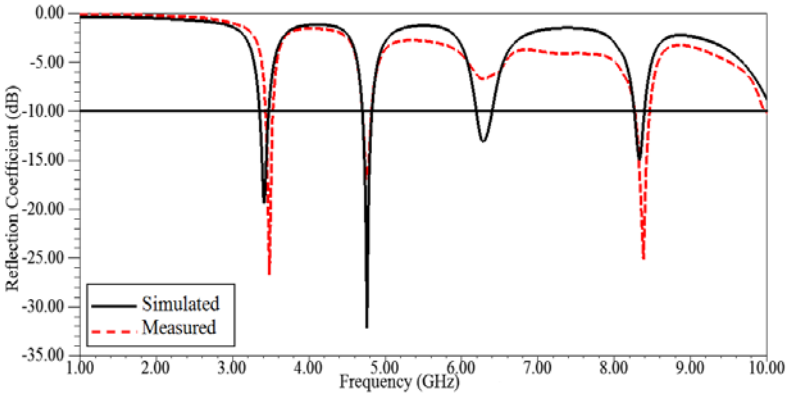

Figure 6. Reflection coefficient versus frequency curve of proposed antenna 1.

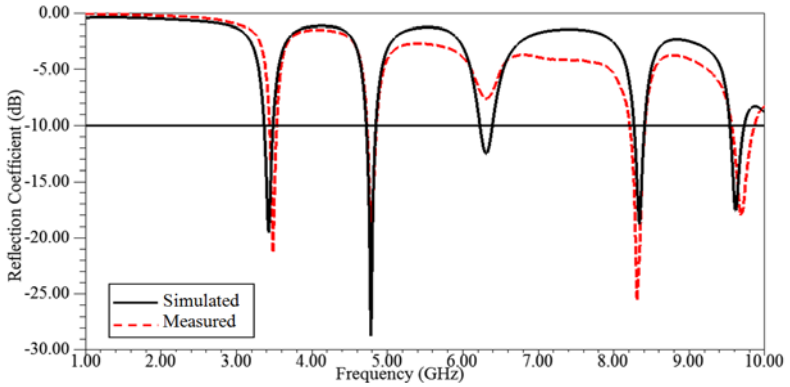

Figure 7. Reflection coefficient versus frequency curve of proposed antenna 2.

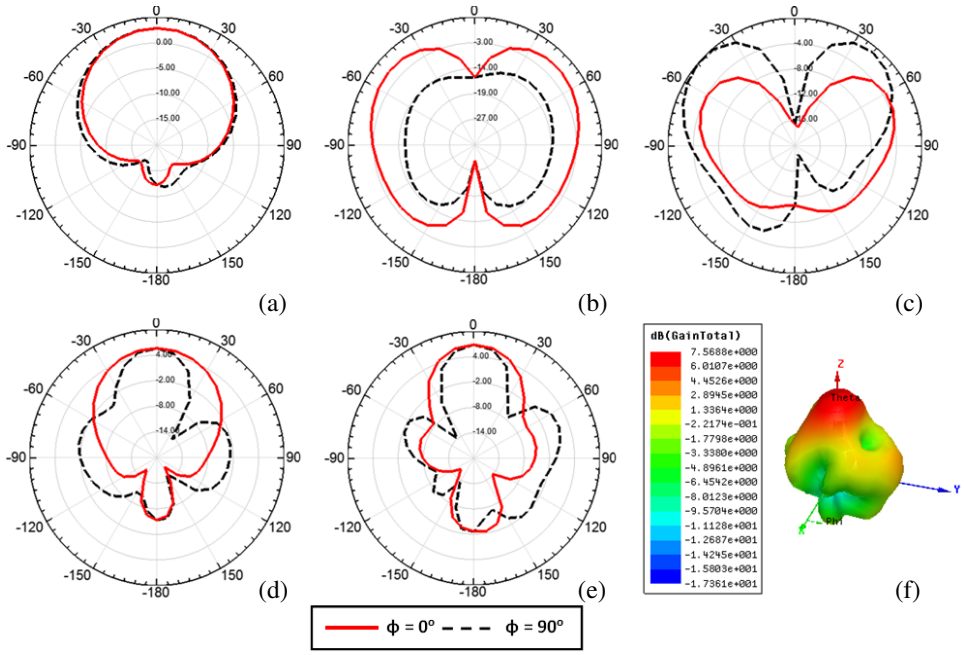

Figure 8. 2D radiation pattern at resonant frequency of (a) 3.43 GHz, (b) 4.78 GHz, (c) 6.32 GHz, (d) 8.34 GHz, (e) 9.64 GHz and (f) 3D gain plot at 9.64 GHz frequency.

Table 4. Comparison of proposed antenna with other published work.

References	Dimensions (mm × mm)	Operating Frequencies (GHz)	Gain (dB)
[4]	2000 × 2000	2.78/4.29	4.45/5.40
[5]	30 × 30	2.05	3.2
[6]	42 × 42	2.49	6.5
[10]	78 × 38	1.54/1.88	–
[13]	100 × 50	1.75/3.0/4.5/6.0	1.35/4.08/4.22/7.34
[14]	70 × 70	2.4	2.3
[15]	22 × 22	4.26	1.67
[21]	50.5 × 83.5	1.1/3.4/5.8	1.74/5.95/4.22
[22]	60 × 20	2.0/5.0	1.8/2.4
[23]	41 × 100	1.8/5.0/6.9	–
[24]	100 × 100	1.42/2.61/3.65/4.93/6.15	2.2/2.2/3.4/4.4/4.0
[25]	50 × 50	2.45/3.4/5.8	–
[26]	80 × 80	3.5–7.02	6.74 (maximum)
[27]	100 × 100	4.7–12.04	8.76 (maximum)
[28]	50 × 50	5.3–10.50	6.56 (maximum)
Proposed work	38.92 × 45	3.41/4.78/6.32/8.34/9.61	2.84/6.90/5.13/5.57/7.56

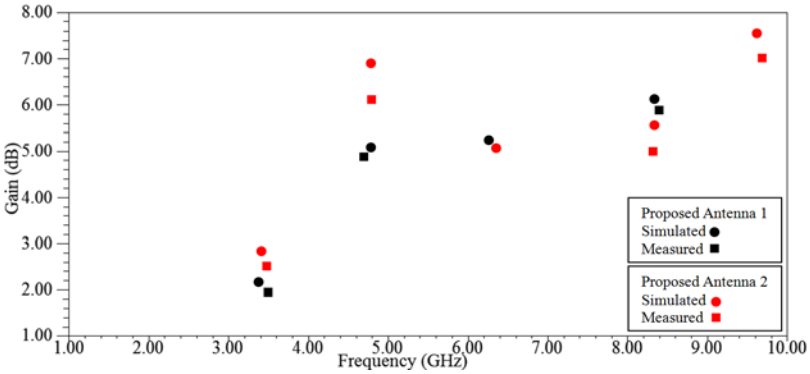

Figure 9. Simulated and measured gain of proposed antenna 1 and 2 at different resonant frequencies.

5. CONCLUSION

A new fractal antenna has been simulated and proposed by combining Minkowski and Sierpinski carpet antennas with area $45 \times 38.92\,\text{mm}^2$ and exhibits multiband characteristics. The simulated antenna covers five bands while fabricated antenna covers four bands for wireless communication. However, this is a reasonable agreement, and the reason for the difference in one frequency band is the reflection from SMA connector and some uncertainty in the electrical properties of the substrate. The proposed antenna is useful for covering four different wireless applications such as Wi-Max (3.43 GHz), C band application (4.78 GHz), point-to-point hi speed wireless (6.32 GHz), X-band applications (8.34 GHz, 9.64 GHz). The proposed hybrid antenna has acceptable value of VSWR, gain and return loss.

REFERENCES

1. Singh, A. and S. Singh, "A novel CPW-fed wideband printed monopole antenna with DGS," *International Journal of Electronics and Communications (AEU)*, Vol. 69, 299–306, 2015, http://dx.doi.org/10.1016/j.aeue2014.09.016.
2. Khandewal, M. K., B. K. Kanaujia, S. Dwari, S. Kumar, and A. K. Gautam, "Analysis and design of dual band compact stacked Microstrip patch antenna with defected ground structure for WLAN/Wi-Max," *International Journal of Electronics and Communications (AEU)*, Vol. 69, 39–47, 2015.
3. Azaro, R., D. Luca, E. Zeni, M. Benedetti, P. Rocca, and A. Massa, "A hybrid prefractal three-band antenna for multistandard mobile wireless applications," *IEEE Antennas and Wireless Propagation Letters*, Vol. 8, 905–908, 2009.
4. Behera, S. and K. J. Vinoy, "Multi-port network approach for the analysis of dual band fractal microstrip antennas," *IEEE Transactions on Antennas and Propagation*, Vol. 60, No. 11, 5100–5106, 2012.
5. Oraizi, H. and S. Hedayati, "Miniaturization of microstrip antennas by the novel application of Guiseppe Peano Fractal Geometries," *IEEE Transactions on Antennas and Propagation*, Vol. 60, No. 8, 3559–3567, 2012.
6. Reddy, V. V. and N. V. S. N. Sarma, "Compact circularly polarized asymmetrical fractal boundary microstrip antenna for wireless applications," *IEEE Antennas and Wireless Propagation Letters*, Vol. 13, 118–121, 2014, doi: 10.1109/LAWP.2013.2296951.
7. Bhatia, S. S., J. S. Sivia, and N. Sharma, "An optimal design of fractal antenna with modified ground structure for wideband applications," *Wireless Personal Communication*, 1–15, 2018. http://dx.doi.org/10.1107/s11277-018-5891-2.
8. Sharma, N. and V. Sharma, "A journey of antenna from dipole to fractal: A review," *International Journal of Engineering Technology*, Vol. 6, 317–351, 2017.
9. Punete, C., B. Aliaada, J. Romeu, and R. Cardama, "On the behavior of Sierpinski multiband antenna," *IEEE Transcation on Antenna Propagation*, Vol. 46, No. 4, 517–524, 1998.
10. Abdullah, N., M. A. Arshad, E. Mohd, and S. A. Hamzah, "Design of Minkowski Fractal Antenna for dual band applications," *Proc. IEEE — Conference on Computer and Communication Engineering*, 352–355, 2015.
11. Sharma, N. and S. S. Bhatia, "Split ring resonator based multiband hybrid fractal antennas for wireless applications," *AEUE — International Journal of Electronics and Communications*, Vol. 93, 39–52, 2018.
12. Gianvittorio, J. P. and Y. R. Samii, "Fractal antennas: A novel antenna miniaturization technique, and applications," *IEEE Antenna's and Propagation Magazine*, Vol. 44, No. 1, 20–36, 2002.
13. Choukiker, Y. K., S. K. Sharma, and S. K. Behera, "Hybrid fractal shape planar Monopole Antenna covering multiband wireless communication with MIMO implementation for handheld mobile devices," *IEEE Transactions on Antennas and Propagation*, Vol. 62, No. 3, 1483–1487, 2014.
14. Orazi, H. and H. Soleimani, "Miniaturization of the triangular patch antenna by the novel dual-reverse-arrow fractal," *IET Microwaves, Antennas & Propagation*, 1–7, 2014, doi: 10.1049/iet-map.2014.0462.
15. Mitra, D., B. Ghosh, A. Sarkhel, and S. R. B. Chaudhuri, "A miniaturized ring slot antenna design with enhanced radiation characteristics," *IEEE Transactions on Antennas and Propagation*, Vol. 64, No. 1, 300–305, 2015.
16. Camps-Raga, B. and N. E. Islam, "Optimized simulation algorithms for fractal generation and analysis," *Progress In Electromagnetics Research M*, Vol. 11, 225–240, 2010.
17. Baliarda, P., "An iterative model for fractal antenna application on the Sierpinski Gasket Antenna," *IEEE Transaction on Antenna and Propagation*, Vol. 48, No. 5, 713–719, 2000.
18. Kumar, Y. and S. Singh, "A compact multiband hybrid fractal antenna for multistandard Mobile wireless applications," *Wireless Pers. Commun.*, Vol. 84, No. 1, 57–67, Springer, April 2015, doi:

10.1007/s11277 -015-2593-x.

19. Bhatia, S. S., A. Sahni, and S. B. Rana, "A novel design of compact monopole antenna with defected ground plane for wideband applications," *Progress In Electromagnetics Research M*, Vol. 70, 21–31, 2018.
20. Karli, R. and H. Ammor, "A simple and original design of multiband microstrip patch antenna for wireless communication," *IJMA*, Vol. 2, No. 2, 41–43, April 2013.
21. Kumar, A., A. Patnaik, and G. Christos, "Design and testing of a multifrequency antenna with a reconfigurable feed," *IEEE Antennas and Wireless Propagation Letters*, Vol. 13, 730–733, April 2014.
22. Luo, Q., J. R. Pereira, and H. M. Salgado, "Fractal monopole antenna for WLAN USB dongle," *Proc. IEEE — Conference on Antenna & Propagation*, 245–247, 2009.
23. Rao, Q. and W. Geyi, "Compact multiband antenna for handheld devices," *IEEE Transactions on Antennas and Propagation*, Vol. 57, No. 10, 3337–3339, 2009.
24. Dhar, S., R. Ghatak, B. Gupta, and D. R. Poddar, "A dielectric resonator loaded Minkowski Fractal shaped slot loop heptaband antenna," *IEEE Transactions on Antenna and Propagation*, 1–9, 2015, doi: 10.1109/TAP.2015.2393869.
25. Reddy, V. V. and N. V. S. N. Sarma, "Tri-band circularly-polarized Koch fractal boundary microstrip antenna for wireless applications," *IEEE Antennas and Wireless Propagation Letters*, 1–4, 2013, doi: 10.1109/LAWP.2014.2327566.
26. Kiran, D. V., D. Sankaranarayanan, and B. Mukherjee, "Compact embedded dual-element rectangular dielectric resonator antenna combining Sierpinski and Minkowski fractals," *IEEE Transactions on Components, Packaging and Manufacturing Technology*, Vol. 7, No. 5, 786–791, 2017.
27. Sankaranarayanan, D., D. Venkatakiran, and B. Mukherjee, "A novel compact fractal ring based cylindrical dielectric resonator antenna for ultra-wideband applications," *Progress In Electromagnetics Research C*, Vol. 67, 71–83, 2016.
28. Gupta, S., P. Kshirsagar, and B. Mukherjee, "Sierpinski fractal inspired inverted pyramidal DRA for wide band applications," *Electromagnetics, Taylor & Francis*, Vol. 38, No. 2, 103–112, 2018.